Earth and Planetary Science Letters 457 (2017) 385–394

Contents lists available at ScienceDirect

Earth and Planetary Science Letters

www.elsevier.com/locate/epsl

Helium and thorium isotope constraints on African dust transport to the Bahamas over recent millennia

Christopher T. Hayes [a,b,*], David McGee [a], Sujoy Mukhopadhyay [c], Edward A. Boyle [a], Adam C. Maloof [d]

[a] Department of Earth, Atmospheric and Planetary Sciences, Massachusetts Institute of Technology, Cambridge, MA, United States
[b] School of Ocean Science and Technology, University of Southern Mississippi, Stennis Space Center, MS, United States
[c] Department of Earth and Planetary Sciences, University of California, Davis, CA, United States
[d] Department of Geosciences, Princeton University, Princeton, NJ, United States

ARTICLE INFO

Article history:
Received 21 June 2016
Received in revised form 23 September 2016
Accepted 16 October 2016
Available online 4 November 2016
Editor: M. Frank

Keywords:
aerosols
mineral dust
thorium isotopes
helium isotopes
Anthropocene
Little Ice Age

ABSTRACT

Despite its potential linkages with North Atlantic climate, the variability in Saharan dust transport to the western North Atlantic over the past two millennia has not been well-characterized. A factor of 4 increase in dust production in sub-Saharan Africa has been attributed to the onset of Sahelian agriculture 200 yr ago. The regional extent of this anthropogenic dust increase, however, remains uncertain. Additionally, while millennial-scale cold periods of the last deglaciation have been associated with strong increases in North African dust emissions, few adequate records exist to observe dustiness during the Little Ice Age, a century-scale cooling of the North Atlantic (AD 1400–1800). In this study, we develop a new technique for the paired use of ^{230}Th-normalized ^{232}Th fluxes and ^{3}He-normalized ^{4}He fluxes in Bahamian tidal flat sediments. After justifying the fact that ^{230}Th and ^{3}He have had relatively constant sources to tidal flat and banktop waters, and accounting for the smoothing effect of bioturbation, a factor of 4 change in far-field dust transport to the western North Atlantic between the pre-industrial and modern era is not supported by our dust proxies over the past 2000 yr. Furthermore, we speculate why the response of western North Atlantic dust deposition associated with the Little Ice Age climate anomalies may have been modest compared to prior climatic events of the early Holocene or the last deglaciation.

1. Introduction

Aerosols constitute one of the largest uncertainties in global climate models, and mineral dust makes up roughly 70% of the global aerosol burden by mass (Tsigaridis et al., 2006). Predictions of future climate scenarios disagree in the magnitude and sign of changes in mineral dust deposition. Thus, we are motivated to provide observational records of dust deposition during past climatic changes to test and refine models of future change. Constraints on dust loads during the last two millennia are particularly lacking, leading to uncertainty as to anthropogenic impacts on dust emissions and aerosol loading used in simulations of preindustrial and last-millennium climate. Because the Sahara is the world's largest source of mineral dust, the North Atlantic Ocean has been a focus of dust time-series investigations. Dust flux has been reconstructed at millennial resolution using deep sea sediments, in particular over the Holocene (Albani et al., 2015, and the references therein). Methods that provide annual-to-sub-annual resolution cover at most the past 5 or 6 decades, such as direct aerosol collection (Prospero and Lamb, 2003), corals (Mukhopadhyay and Kreycik, 2008) or satellite optical depth (Evan et al., 2011). In this study, we seek to fill this temporal gap between the instrumental period and the late Holocene using sedimentary records from a Bahamian tidal flat.

A Mauritanian shelf sediment core (Mulitza et al., 2010) demonstrates a factor of four increase in eolian dust deposition beginning at the intensification of agriculture in the Sahel 200 yr ago. The inference of anthropogenic influence is consistent with concurrent observations of deforestation over the past 50 yr and increased land use concurrent with increases in dust production in the Senegal River basin (Niang et al., 2008). Based in part on this study, some models assume that preindustrial dust loading was only 50% of modern dust loading (e.g., Albani et al., 2014). However, anthropogenic dust emissions from North Africa, coming largely from the Sahel, account for only 15% of total North African dust emissions, which are dominated by natural emissions from

* Corresponding author at: School of Ocean Science and Technology, University of Southern Mississippi, Stennis Space Center, MS, United States.
E-mail address: Christopher.t.hayes@usm.edu (C.T. Hayes).

http://dx.doi.org/10.1016/j.epsl.2016.10.031
0012-821X/

the Sahara (Ginoux et al., 2012). Additionally, much of the anthropogenic increase seen on the Mauritanian shelf was due to dust of large grain-size (>10 μm) (Mulitza et al., 2010). Only very fine dust (<5 μm) is exported out into the western Atlantic (Muhs et al., 2007; Reid et al., 2003). Furthermore, a model reanalysis suggests that dust optical depth over the North Atlantic was close to its present value in AD 1850 (Evan et al., 2016) and a study in the Everglades of South Florida found no change in the concentration of quartz grains, taken to represent Saharan dust, over the past 2800 yr (Glaser et al., 2013).

There is a seasonal aspect for expecting dust deposition very close to the source to differ from that in the far-field North Atlantic. The Bahamas area receives Saharan dust predominantly in summer (Prospero, 1999) due to the seasonal movement of the Intertropical Convergence Zone (ITCZ). In summer, the northward excursion of the trade winds at the northern boundary of the ITCZ acts to both increase Saharan dust emissions as well as to facilitate trans-Atlantic dust transport to more northerly (20–30°N) destinations (Rodríguez et al., 2015). In contrast, in winter with the ITCZ further south, total African dust emissions are reduced and eastward dust transport occurs mostly at latitudes south of 15°N. For these reasons, we expect the modern increase in Sahel dust production was not representative of changes in the Bahamas and the western North Atlantic region.

On longer timescales, millennial variations in North Atlantic dust deposition have been documented back through the last ice age. Records of Holocene and last glacial variability in Saharan dust has been limited mostly to deep ocean sedimentary records. Periods of pronounced (several degrees Celsius) cooling in the North Atlantic region, such as Heinrich Stadial 1 (15–18 ka) and the Younger Dryas (12–13 ka), have been associated with increases in African dust emissions to roughly 2–3 times modern levels (McGee et al., 2013, and the references therein). Furthermore, the Early Holocene African Humid Period (5–11.7 ka) has been characterized by dust fluxes on the West African margin that were a factor of 2–5 lower than modern (McGee et al., 2013). Since the end of the African Humid Period, there is evidence for a further, gradual aridification of tropical Africa over the past 3000 yr from the Mauritanian shelf dust record (Mulitza et al., 2010), continental precipitation records (Shanahan et al., 2015), and reduced Niger river outflow (Weldeab et al., 2007).

A general mechanism has been proposed for these variations, applicable to modern inter-annual variability as well, involving the meridional sea-surface temperature and/or pressure gradients in the Atlantic and the position of the ITCZ over the African continent (e.g., Evan et al., 2011; Rodríguez et al., 2015). The present Andros Island records offer an opportunity to test the coherence of African dust and North Atlantic climate over the Little Ice Age. This period (roughly 1400 to 1800 AD) has been characterized by a modest cooling (~0.5 °C) found most strikingly in the extratropical Northern Hemisphere continents (Mann et al., 2009).

2. Approach

Our approach to reconstructing dust input here is geochemical. Thorium and helium share a unique property in that both elements have a dominant isotope (^{232}Th and ^{4}He) associated with aerosol mineral dust and a minor isotope (^{230}Th and ^{3}He) that has a relatively constant source to the ocean. In the case of ^{230}Th, the current study is a novel application in that normally the use of sedimentary ^{230}Th as a normalizing factor is restricted to ocean water depths in excess of a few hundred meters, where a large, predictable inventory of ^{230}Th, scavenged from water column decay of ^{234}U, has developed. On the tidal flat, in shallow water (<1 m), or even on a tidal channel level crest above mean tide level, the source of ^{230}Th in the sediments is likely dominated by release from banktop pore waters (Robinson et al., 2004), as described later in this section. In the case of ^{3}He, the dominant source is atmospheric deposition of interplanetary dust particles highly enriched in ^{3}He. This extraterrestrial ^{3}He supply has had indistinguishable and constant rates in equatorial deep-sea sediments and polar ice caps over the Late Quaternary (McGee and Mukhopadhyay, 2013, and the references therein), supporting the expectation of constant supply to this shallow water setting.

In the Triple Goose Creek area of Andros Island (Fig. 1), we have cored within a well-studied system of beach ridges, tidal channels, levee crests and mangrove ponds abutting an inland algal marsh (Hardie, 1977; Maloof and Grotzinger, 2012; Shinn et al., 1969). The carbonate particles accumulating here are primarily derived from aragonite-producing marine algae on the Great Bahama Bank and subsequently are washed inshore by tides. The levees are built up by overbank flooding and the low ponds are normally flooded twice daily by tides with a range of roughly 40 cm (Hardie, 1977). The dust concentrations recorded in these accumulating sediments therefore reflect the interplay of dust deposited from the local atmosphere, dilution by the dominant carbonate sediments, and dust swept in by the tides from the shallow (~3 m water depth) Great Bahama Bank.

Our goal is to reconstruct atmospheric deposition from the bulk sediment record. Therefore, we need a way to correct for temporal variations in carbonate dilution and lateral addition of dust. Fortunately, any ^{232}Th and ^{4}He supplied to a core site laterally from the bank top should also be accompanied by a proportional amount of ^{230}Th and ^{3}He. This is an assumption that deserves critical evaluation, which we present in the following paragraphs of this section. Less controversially, dilution will affect all these isotopes equally. Thus, the two ratios ^{232}Th/^{230}Th and ^{4}He/^{3}He provide proxies of atmospheric dust input that account for possible changes in lateral addition with time. The lateral addition of sediments is termed sediment focusing, and the magnitude of sediment focusing can be expressed as a focusing factor (F): the ratio of the total accumulation rate of the isotope in question to its local production, or deposition, rate.

In the case of ^{230}Th, its production in water over the Great Bahama Bank consists of two sources. The first is the strictly known production from the decay of dissolved ^{234}U in seawater. As mentioned, in the deep ocean this source predominates, but in such a shallow setting as the tidal flat, another source is likely to be much larger. This second source is release of ^{230}Th from sediment porewaters derived from ^{234}U decay within the high U (~3 ppm, Fig. 2) aragonite sediments and supplied to porewaters by recoil associated with alpha decay. Robinson et al. (2004) found evidence for this benthic source in that banktop water had much higher ^{230}Th content than at similar depths in the surrounding deep ocean. Using a box-model approach with reasonable assumptions, these authors determined the ^{230}Th supply from the sediments to the overlying water could easily be 30 times the in-situ production in the water column above the bank. There have been no independent determinations of this flux. Without precisely knowing the benthic supply of ^{230}Th, we cannot make quantitative estimates of sedimentary fluxes as is done using ^{230}Th-normalization in deep ocean studies (Francois et al., 2004). Nonetheless, we do expect the benthic ^{230}Th flux to be constant over the timescales considered in this study. Our justification of this expectation is as follows. The uranium content of the banktop sediments is largely set by its authigenic incorporation into aragonite. This is a factor that is not likely to change on a millennial timescale. Additionally, variability in the processes that lead to pore water release of ^{230}Th, such as sediment resuspension and hydraulic flow within the porous Great Bahama Bank, is likely controlled by stochastic physical forces. Again, at least on centennial- to millennial-timescales, in the absence of evidence for changes in the long-term averages of these

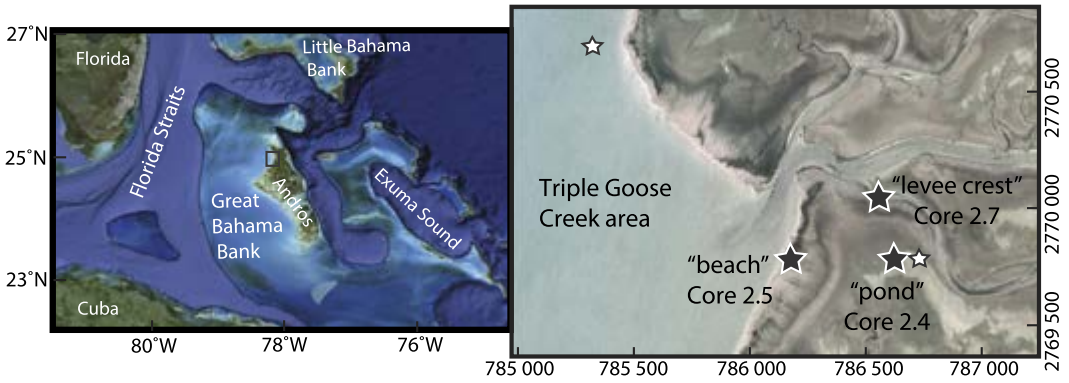

Fig. 1. Study site locations based on maps extracted from Google Earth Pro. The overview map on the left is based on a Landsat image, using data from SIO, NOAA, U.S. Navy, NGA and GEBCO. The detailed map on the right, which is located roughly in the black box indicated in the overview map, is from DigitalGlobe © 2014. Coordinates on the detailed map are in kilometers and refer to UTM grid 17R. The black stars indicate sediment coring locations and the small white stars indicate water sampling locations.

physical forces, we expect banktop environments to experience a relatively constant release of porewater ^{230}Th averaged over the large expanse of the Great Bahamas Bank. Thus, while we are not able to determine an absolute focusing factor with ^{230}Th, we can use it as a normalizing factor to account for relative changes in sediment focusing based on the assumption of its constant release to pore waters.

Once in the dissolved phase, due to its insoluble nature, ^{230}Th in the banktop waters is expected to be rapidly adsorbed (or scavenged) onto the abundant carbonate particles with a residence time of less than six months (Robinson et al., 2004). The same is true for any ^{232}Th that dissolves from dust, as it is estimated that 5–20% of aerosol ^{232}Th dissolves in the upper water column (Hayes et al., 2013). Thus, ^{232}Th delivery to the Andros Island cores consists of both structurally-intact Saharan dust, as well as scavenged ^{232}Th on the carbonate mud.

As a noble gas, He in the sediments is fully contained in crystalline particles, in contrast to sedimentary Th, which has a fraction that dissolves and spends some time (months) in the water before being adsorbed and buried. In the helium system, at least during the Quaternary, ^{3}He is largely supplied to the Earth surface in the form of a relatively constant rain of interplanetary dust particles (IDPs). Its rain to Earth is calculated from its accumulation in deep sea sediments and ice cores, averaged over timescales ranging from 10^6 yr to the Holocene. These estimates range from 4 to 13 $\times$ 10^{-9} cc (pcc) ^{3}He at STP per m^2 per year, and most are consistent with 8 $\pm$ 3 pcc/m^2/yr (McGee and Mukhopadhyay, 2013). Thus, without a proper regional calibration, we can only be confident in the absolute ^{3}He input to our sites to within ~50%. Nonetheless, the constancy of IDP rain into Holocene and Glacial-aged ice cores (Brook et al., 2009, 2000; Winckler and Fischer, 2006) supports the view that the ^{3}He flux over the Bahamas has remained relatively constant throughout the past two millennia. Furthermore, if we assume the 8 $\pm$ 3 pcc/m^2/yr ^{3}He$_{ET}$ deposition rate is correct, this affords us an estimate of the focusing factor (F) in the sediments. Focusing factors are calculated as bulk averages between dated depth horizons, since it cannot generally be assumed that mass accumulation rates are constant between age controls. F equal to 1 implies no focusing, greater than 1 implies focusing and less than 1 implies sediment winnowing or that sediments have been removed.

3. Material and methods

3.1. Coring and core descriptions

Fieldwork took place during March 2014 in the Triple Goose Creek area on northwest Andros Island in the Bahamas (Fig. 1).

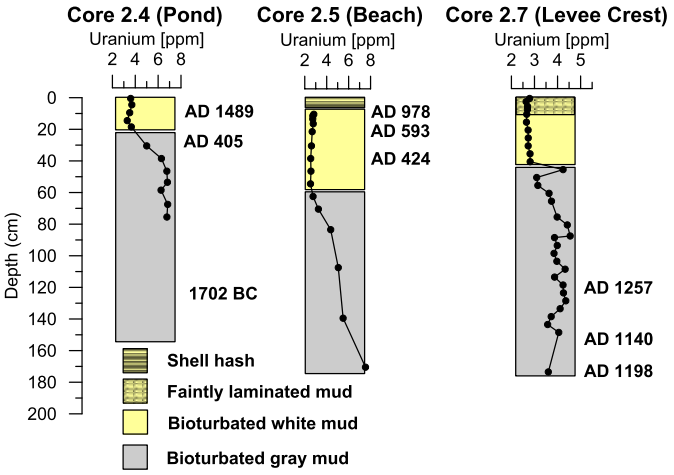

Fig. 2. Visual description of the Andros Island sediment cores. Overlaid on each core is the depth profile of sedimentary uranium concentrations. To the right of each core is indicated the calibrated (Marine13) radiocarbon dates in calendar years positioned at the depth of foraminifera samples used for dating. A 400 $\pm$ 70 yr reservoir correction has been applied to the measured ages.

Sediment cores were collected using a 5 cm diameter, stainless steel and aluminum Livingstone piston corer from the University of Minnesota Limnological Research Center. Extruded cores were split open on plastic sheets in the field and sampled at cm-scale resolution. The corer was 1 m in length. Cores of 1.5–2 m were taken by re-entering the hole created by a first core. We use a composite depth scale for the core as a whole, assigning a depth to the top of the second core equal to the full length of the first core.

We chose three coring sites (Fig. 1): a mangrove pond in roughly 1 m of water (Core 2.4), a beach at the western edge of the tidal flat, about 60 cm above mean-tide level (Core 2.5) and a levee crest at the edge of a tidal channel, about 40 cm above mean-tide level (Core 2.7). We refer to these as the Pond, Beach and Levee Crest cores throughout the manuscript. All cores consisted of calcium carbonate mud (>94% by weight) bioturbated by gastropods and polychaete worms. The remaining, percent-level, components of the sediments were organic matter, largely in the form of decaying mangrove roots, and aluminosilicates taken to be Saharan mineral dust. Due to the strong transport of the Gulf Stream in the Florida Straits, Andros Island is well-isolated from continental input from Florida, making transported Saharan dust the only non-local source of sediments (Muhs et al., 2007).

All cores contained a stark transition with depth from white mud to gray mud (Fig. 2) which marks the transition from oxic to sulfidic conditions (Maloof et al., 2007). This redox transition is

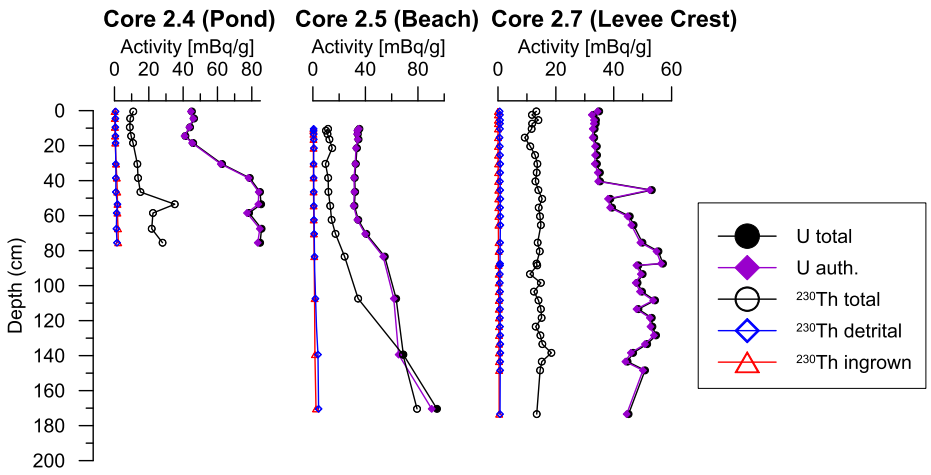

Fig. 3. Depth profiles of U and ^{230}Th activities in the Andros Island sediment cores. Total uranium and ^{230}Th are as measured. Authigenic uranium (U auth.) is estimated by subtracting a detrital component based on measured ^{232}Th. Detrital ^{230}Th is estimated similarly. Ingrown ^{230}Th is based on decay of U auth. since the time of deposition.

well marked by the enrichment of uranium (Fig. 2) as uranium becomes insoluble and precipitates in the sulfidic conditions. Reducing conditions at depth draw dissolved U from above down a gradient in dissolved U concentrations in porewaters (Klinkhammer and Palmer, 1991). The depth of this redox transition in the cores reflects the position of mean-tide level throughout the area (Maloof and Grotzinger, 2012). In the Beach core, the upper 8 cm consisted of broken shell hash, a product of the much stronger tidal energy available in this location. Below 8 cm, however, the core material was bioturbated mud, indicating that this location was once a pond environment in times of lower sea level (Maloof and Grotzinger, 2012). In the Levee Crest core, the upper 20 cm of white mud contains faint laminations, suggesting reduced bioturbation in this section. We also took water samples from a Pond and the banktop for Th isotope analysis (see Supplemental Material for protocols).

3.2. Radiocarbon and excess lead-210

The benthic foraminifera *Peneroplis proteus* are abundant in the study area (Shinn et al., 1969), and were picked from sediments sieved at 355 μm, washed and sonicated in Milli-Q water, and dried at 80 °C. Radiocarbon measurements were performed on 5 mg foraminifera samples at the Center for Accelerator Mass Spectrometry, Lawrence Livermore National Laboratory. See Supplemental Material for details on calendar age conversion and reservoir age estimates.

Gamma spectroscopy was performed at MIT to analyze sedimentary excess (xs) ^{210}Pb. Sourced from atmospheric deposition, its radioactive decay with depth in the sediment can be used to corroborate the radiocarbon dating. See Supplemental Materials for further analytical procedures.

3.3. Thorium and helium derived parameters

Uranium, thorium and helium isotope analyses were performed by mass spectrometry after sample preparation following modifications of published methods (Gayer et al., 2008; McGee et al., 2013). Full procedures are included in the Supplemental Material. We make small corrections to the ^{230}Th data to account for detrital input and ingrowth and decay within the sediments to calculate the initial, excess $^{230}Th_{xs,0}$. This tidal flat Th/U data is quite distinct from typical pelagic data. For instance, in terms of activity, the bulk ^{230}Th in the sediments (10–30 mBq/g) is not in excess of the bulk ^{238}U (40–80 mBq/g) (Fig. 3). Nearly all (>95%) of this ^{238}U, however, is authigenic (see Supplemental Material) and we assume authigenic U is not in secular equilibrium with ^{230}Th, but only contributes "ingrown" ^{230}Th, from ^{234}U decay for as long as the sediments have been buried. Accumulation of ^{230}Th from the decay of authigenic ^{234}U (assumed present at the seawater ^{234}U/^{238}U ratio) is calculated based on the depositional age of the sediments, amounting to a 3% correction, on average for the samples studied (range 0–13%). Detrital ^{230}Th present in the sediments is assumed to come from Saharan dust, which based on near crustal ^{230}Th/^{232}Th ratios and measured ^{232}Th, is also small, at the percent level. Similarly, the He isotopic data is corrected (also at the percent level) to isolate the fraction of total ^{3}He from IDPs ($^{3}He_{ET}$) and the fraction of total ^{4}He from dust ($^{4}He_{TERR}$). Full descriptions of these corrections are presented in the Supplemental Material.

The ^{232}Th concentration of fine-grained (<5 μm) Saharan dust in the Caribbean is 13.7 ± 1.2 μg/g (Muhs et al., 2007). In this study, we undertook new measurements of ^{4}He in Northwest Providence Channel sediments whose dust content has been determined using ^{232}Th (Williams et al., in press), core OCE205-2 103GGC (26°04′ N, 78°03′ W; 965 m water depth) on the south flank of the Little Bahama Bank (see Fig. 1). From measured $^{4}He_{Terr}$/^{232}Th ratios of 105, 96 and 64 mcc STP/g in samples of age 2.7, 3.3 and 4.1 ka, respectively, we infer that the fine grained Saharan dust reaching Andros Island has a ^{4}He concentration of 1212 ± 294 ncc/g. These ^{4}He concentrations and ^{4}He/^{232}Th ratios are very similar to values found for the <5 μm fraction of dust source area samples from Australia, East Asia and South America (800–2000 ncc/g ^{4}He and ~50–250 mcc/g ^{4}He/^{232}Th, respectively) (McGee et al., 2016). This ^{4}He concentration for dust deposited in the Bahamas is much lower than concentrations of 5626 ± 3205 ncc/g found on the African margin in Cape Blanc sediments (Mukhopadhyay and Kreycik, 2008), consistent with the grain-size effect on ^{4}He concentration found by McGee et al. (2016).

4. Results

4.1. Core chronologies: ^{14}C

The Pond and Beach cores demonstrate stratigraphic order in their foraminifera ages, based on ^{14}C ages (Fig. 4), but their core tops appear to be significantly older than modern.

For the Pond core, the sedimentation rate implied by the dates at 7 cm and 32.5 cm is 0.235 ± 0.037 mm/yr. This sedimentation rate indicates a coretop (depth = 0 cm) age of AD 1787 ± 82. Therefore, roughly 225 yr of sedimentation (~5.5 cm at the assumed rate) may have been lost due to disturbance/compaction

Table 1
Radiocarbon data and calibration using Marine13, including a reservoir age correction of 400 ± 70 yr, for the Andros Island cores. Radiocarbon age in years before 1950 is quoted using the Libby half-life of 5568 yr. $\delta^{13}C$ values were assumed to be −1 ± 2‰ (VPDB) and this error is accounted for in the reported ^{14}C age.

Core	Composite depth (cm)	^{14}C age (yr)	±	Median probability age (yr AD/BC)	±1σ (yr)
2.4 (Pond)	9–10	840	30	1489	63/71
	31–34	1985	30	405	108/91
	122–125	3725	35	−1702	101/111
2.5 (Beach)	10–12	1420	35	978	83/90
	17–21	1805	30	593	84/72
	39–42	1970	30	424	110/83
2.7 (Levee Crest)	119–123	1135	30	1257	66/71
	149–153	1265	30	1140	75/80
	174–177	1200	35	1198	86/68

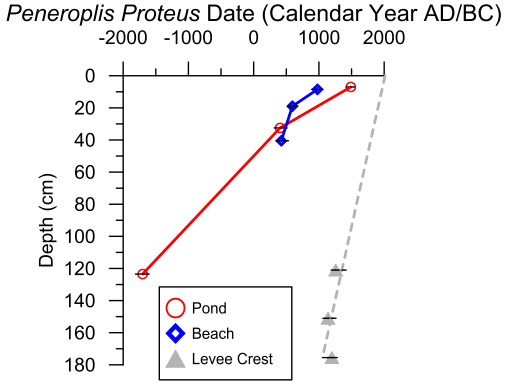

Fig. 4. Calibrated (Marine13) radiocarbon dates based on the benthic foraminifera *Peneroplis proteus* found in each of the three Andros Island cores. A 400 ± 70 yr reservoir correction has been applied to the measured ages. For the Pond and Beach core age models, linear interpolation between dated depth horizons is used. For the Levee Crest core, the age model, shown in gray, is a line drawn between the modern core top (depth 0 cm = year AD 2014) and the average depth and average age of the three measured samples.

during core collection, or due to natural processes associated with water movements in the pond.

The sedimentation rate in the Beach core between 9 cm and 19 cm is 0.260 ± 0.098 mm/yr, similar to the Pond core. This rate implies a core top age of AD 1325 ± 157, indicating that a much larger amount of sediment has been eroded away here by wave and storm action (as evidenced by the abrupt upward transition from mud to coquina) associated with the development of the beach environment as local sea level rises.

The fact that most of the foraminifera ages in both the Pond and Beach cores are older than AD 700 is surprising in itself, in consideration of previous work. Maloof and Grotzinger (2012) found that *Peneroplis* specimens within the basal unit of 5 cores throughout the Triple Goose Creek area dated to AD 700–1005, averaging AD 903. Since the Bahama Banks were flooded by rising Holocene sea-level around 4500 ± 1000 yr ago (or ~2500 ± 1000 BC) (Slowey and Henderson, 2011), there may have been a several thousand year energetic period between initial inundation of the region and the beginning of quiescent pond-like sedimentation. Based on the bottom date of the Pond core, however, pond sedimentation may have begun as early as 1702 BC in that location. In the Beach core, the sedimentation rate between 19 and 40.5 cm depth (1.27 mm/yr), implies a core-bottom (170 cm) date of 600 BC.

Virtually all of the cores described by Maloof and Grotzinger (2012) were collected further inland than the Pond and Beach locations. We speculate that the older bottom dates reported here suggest that these locations were among the first to develop undisturbed sedimentation, perhaps due to details of the topography of the underlying cemented Pleistocene reef bedrock. In the age models for these cores, we linearly interpolate age, assuming constant sedimentation rates between dated depth horizons (Fig. 4), with the understanding that continuous sedimentation may be a tenuous assumption in sections much older than AD 700. Further stratigraphic and sedimentological work is needed to clearly define the nature of sedimentation prior to this time, and we focus on the results from the last millennium here.

Foraminifera dates for the Levee Crest were all from the lower 60 cm of this site's 180 cm core. Only in this lower section was foraminifera abundance adequate. These three dates are not in stratigraphic order (Figs. 2, 3, Table 1), but they are consistent with each other within dating uncertainties. The apparent age-inversion may be due to bioturbational mixing. Taking the average depth and average age of the dated foraminifera in this core, and assuming a modern age for the core top (AD 2014 at depth 0 cm) yields a sedimentation rate of 1.83 ± 0.35 mm/yr. This sedimentation rate is consistent with the radiocarbon dating of previous cores (Maloof and Grotzinger, 2012). Noting the old core-top ages found in the Pond and Beach cores, however, the assumption of modern core top is highly uncertain. We therefore analyzed the sediment profiles for unsupported ^{210}Pb which, as described next, corroborates the radiocarbon-based sedimentation rate, supports a modern core top age and provides an estimate of the depth-scale of bioturbation for the Levee Crest core.

4.2. Core chronologies: ^{210}Pb

The shape of the $^{210}Pb_{xs}$ profile in the sediment is affected by biological mixing, age decay during burial and, possibly, changes in sedimentation rate with depth. Ignoring changes in sediment porosity and assuming a constant sedimentation rate (w), $^{210}Pb_{xs}$ activity (A) can be modeled as a function at steady-state of depth (z), diffusional bioturbation rate (D), and radioactive decay constant (λ) (Eq. (1)).

$$D\frac{d^2A}{dz^2} - w\frac{dA}{dz} - \lambda A = 0 \tag{1}$$

The coretop activity (A_o) decays to A at depth z (Eqs. (2), (3)). λ for ^{210}Pb is 0.031223 yr^{-1}.

$$\ln(A/A_o) = \frac{w - \sqrt{w^2 + 4D\lambda}}{2D}z \tag{2}$$

$$\ln(A/A_o) = \frac{-\lambda}{w}z \tag{3}$$

If there were no bioturbational mixing ($D = 0$), the $^{210}Pb_{xs}$ profile of the Levee Crest core (Fig. 5) would imply a sedimentation rate of 2.21 mm/yr using Eq. (3). Assuming, however, that the ^{14}C-based sedimentation rate ($w = 1.83$ mm/yr) is correct, by solving

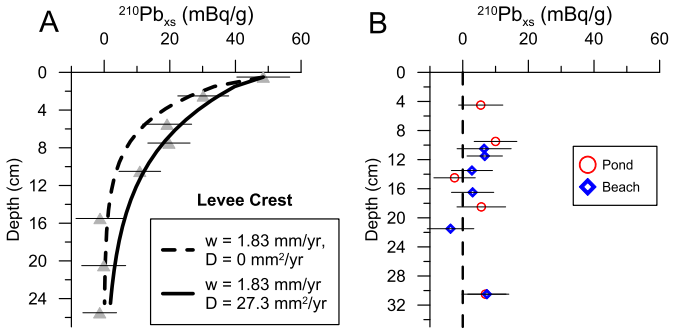

Fig. 5. Excess lead-210 depth profiles in the Andros Island cores. Data from the Levee Crest core is shown in detail in (A) and fit with models of exponential decay following sedimentation rates (w) and varying degrees of sediment diffusivity due to bioturbation (D). In (B), the Pond and Beach cores showed negligible excess ^{210}Pb in the upper 30 cm, indicating core tops older than at least 200 yr. The upper 8 cm of the Beach core consisted of shell hash and therefore samples for ^{210}Pb were taken only below this section in the bioturbated mud (Fig. 2).

Eq. (2), this core has a diffusion rate of 27.3 mm^2/yr. This is a lower than but reasonable diffusion rate compared to that found in 5 m water depth on the Little Bahama Bank of 106 ± 16 mm^2/yr (Henderson et al., 1999). Additionally, we expected reduced bioturbation in the upper section of this core based upon its faint laminations (Fig. 2). Thus the ^{210}Pb results corroborate the ^{14}C-derived sedimentation rate of 1.83 mm/yr.

Annual ^{210}Pb deposition to Bermuda is 115 Bq/m^2 (Turekian et al., 1983), similar to the model-based prediction of deposition to the Bahamas (100–150 Bq/mv^2/yr) (Preiss and Genthon, 1997). Additionally, we can infer the local ^{210}Pb deposition rate by integrating its depth profile (Fig. 5), assuming a dry bulk sediment density (ρ) of 1.14 g/cm^3, as measured on the Little Bahama Bank (Henderson et al., 1999). The total inventory of $^{210}Pb_{xs}$ in the Levee Crest core is 3260 ± 70 Bq/m^2. To support a steady-state against the radioactive decay of the measured inventories would require an input by atmospheric deposition of 102 ± 2 Bq/m^2/yr. If we assume a modern (AD 2014) age for the coretop, using the local atmospheric $^{210}Pb_{xs}$ deposition rate, the coretop $^{210}Pb_{xs}$ activity of 48.5 ± 8.1 mBq/g (Fig. 5) can be used to derive a sediment mass accumulation rate (MAR) (MAR = atmospheric $^{210}Pb_{xs}$ deposition ÷ coretop $^{210}Pb_{xs}$ activity). This calculation gives a sediment MAR of 2100 ± 350 g/m^2/yr.

The sediment MAR based on the ^{14}C-derived sedimentation rate (1.83 ± 0.35 mm/yr), multiplied by the assumed $\rho = 1.14$ g/cm^3 gives 2085 ± 399 g/m^2/yr. That these two independent MAR estimates (2100 and 2085 g/m^2/yr) agree well within uncertainties is a good indication for a modern core top age for the Levee Crest core.

While the $^{210}Pb_{xs}$ profile of the Levee Crest core came from a faintly laminated section, we use the depth of $^{210}Pb_{xs}$ penetration to constrain a lower limit on the sediment mixed layer to 10–12 cm. Using the 1.83 mm/yr sedimentation rate, this mixing depth translates to a bioturbational smoothing in temporal space of about 60 yr for the Levee Crest core. Sediments from the Pond and Beach locations are old enough that all of their $^{210}Pb_{xs}$ has decayed away (Fig. 5). Nonetheless, assuming a similar depth of bioturbation, the lower sedimentation rates from those cores (~0.25 mm/yr) imply longer temporal smoothing (~400 yr). These smoothing time-scales should be considered lower limits.

4.3. Dust proxies

The He and Th isotope concentration data are presented as a function of calendar year in Fig. 6. All four isotopes show a decline in concentrations of roughly a factor of 5 between 500 BC and AD 500, followed by relatively uniform values between AD 500 and

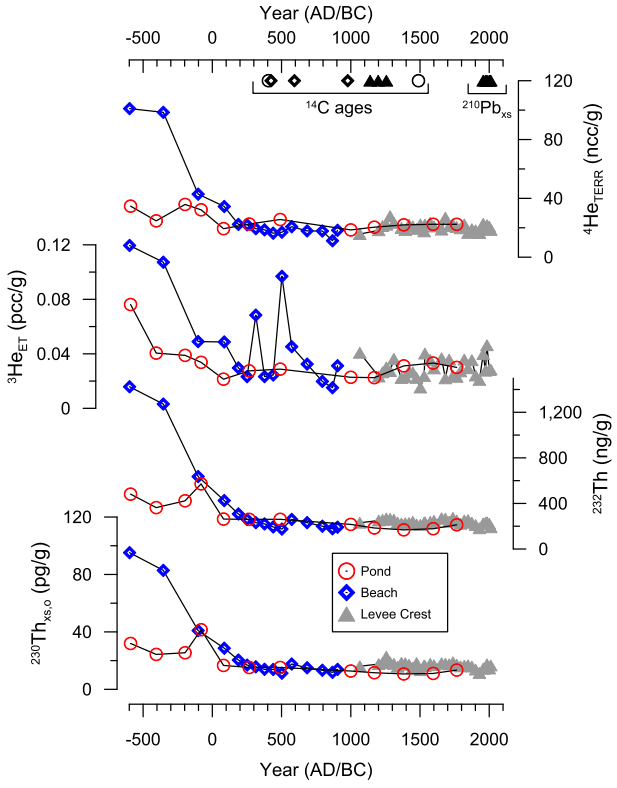

Fig. 6. Sedimentary concentrations (from the top panel to the bottom) of terrigenous helium-4, extraterrestrial helium-3, thorium-232, and initial, excess thorium-230.

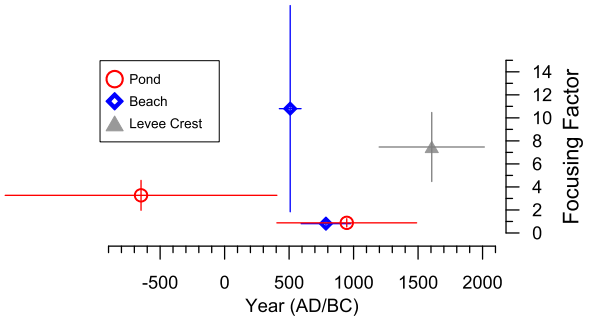

Fig. 7. Focusing factors for the Andros Island cores. These factors are calculated using the inventory of $^3He_{ET}$ within dated depth horizons (indicated by the x-axis errors bars) compared to the global $^3He_{ET}$ deposition of 8 ± 3 pcc/m^2/yr. The uncertainty in the focusing factor is propagated from the uncertainties in the radiocarbon dates, the helium inventories, and the assumed $^3He_{ET}$ deposition rate.

2014. The Beach core shows some spikes in $^3He_{ET}$ at AD 200 and 500 that may represent the sampling of rare high-^{3}He IDPs in the relatively small 1 g samples (Farley et al., 1997).

On the basis of the dust indicators ^{232}Th and $^4He_{TERR}$ alone, one might have interpreted these records to reflect much higher dust input to the Bahamas prior to AD 500. Because our constant-flux proxies $^{230}Th_{xs,o}$ and $^3He_{ET}$ change in concert with the dust indicators, however, it appears that these sites received a relatively stable input of dust throughout. The increased concentrations prior to the Common Era likely reflect less total carbonate accumulation (thus reducing the dilution of the dust). This change may have coincided with a change in sediment focusing, although of course the focusing factors we can estimate are highly age-model dependent (Fig. 7). In the Pond and Beach cores, the post-AD 500 focusing factors are within 10% of 1.0, while prior to this F = 11 ± 9 for the beach core and 3.3 ± 1.3 in the pond core, perhaps indicating that these were higher energy sedimentation environments before

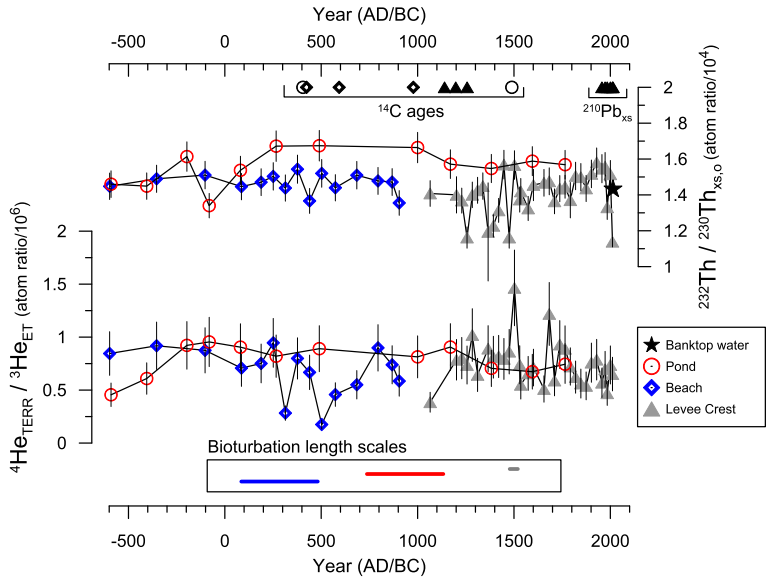

Fig. 8. Dust flux proxy data based on thorium and helium isotope ratio data (units are atom ratios divided by 10^4 and 10^6, respectively) for the Andros Island cores. In the top panel, shown as a star, is the average ^{232}Th/^{230}Th ratio of dissolved Th from two Pond and banktop water samples. The approximate range of temporal smoothing due to bioturbation in the cores is indicated in the bottom panel, 60 yr for the Levee Crest Core and 400 yr for the Pond and Beach cores.

pond-like sedimentation set in. On the Levee Crest, $F = 7.5 \pm 3.0$, and the stability in He and Th concentrations in this core suggests that focusing did not significantly change at this site for the past millennium.

We present the time series of the dust flux proxy ratios ^{232}Th/^{230}Th$_{xs,o}$ and ^{4}He$_{TERR}$/^{3}He$_{ET}$ in Fig. 8. These ratios are linearly related to ^{230}Th$_{xs,o}$-normalized ^{232}Th rain rates and ^{3}He$_{ET}$-normalized ^{4}He$_{TERR}$ rain rates, respectively, on the assumption of a constant supply of ^{230}Th or ^{3}He. The Th ratios have quite a limited range with a relative standard deviation (RSD) among the data from all cores of 8%. The He ratios have a RSD of 28% in all the data, and this lowers to 19% when the five ratios furthest from the mean are excluded. A similar average (720,000) and RSD (30%) of ^{4}He$_{TERR}$/^{3}He$_{ET}$ ratios was found in another core collected in the same area in 2003 that had a bottom age of 1000 AD (Bhattacharya, 2012).

Let us consider what dust flux is implied simply from the MAR of ^{232}Th in the Levee Crest core (since this core overlaps with the instrumental period). We focus on ^{232}Th accumulation because its concentration in fine-grained (<5 μm) Saharan dust (13.7 ± 1.2 μg/g, Muhs et al., 2007) is known more precisely than ^{4}He$_{TERR}$ (1212 ± 294 ncc/g, reported here). Using the average values in the upper 7.5 cm of the core (nominally representing AD 2014–1973), and a dry bulk density of 1.14 g/cm^3, the ^{232}Th MAR is 456 ± 40 μg/m^2/yr, translating to a Saharan dust MAR of 33 ± 4 g/m^2/yr. Recall that this estimate includes both direct atmospheric deposition as well as sediment focusing. Accounting for the focusing factor in this core (7.5 ± 3.0), the estimated Saharan dust deposition is 4.4 ± 1.8 g/m^2/yr.

Available observations from rain collections in nearby South Florida (1982–1984 and 1994–1996) (Prospero et al., 2010, 1987) suggest an average dust deposition in this region of 1.3 g/m^2/yr, or roughly 3 times smaller than what was calculated in our core above. The most uncertain figure in our dust deposition calculation is the assumed ^{3}He$_{ET}$ deposition to calculate the focusing factor (8 ± 3 pcc/m^2/yr). Turning the problem around, the ^{3}He$_{ET}$ deposition to our site would have to be about 3 times lower than the global average in order to make dust deposition in our core exactly equal the modern rate of 1.3 g/m^2/yr. Lower ^{3}He$_{ET}$ inputs at this site relative to the late Quaternary global mean may reflect temporal or spatial variability in IDP fluxes. While this is speculative, there is a possible justification of lower than global average ^{3}He$_{ET}$ fluxes here in the subtropics, as other aerosol-bound isotopes of atmospheric origin, such as ^{10}Be or ^{90}Sr, are known to be transported out of the subtropics by atmospheric circulation to be preferentially rained out in the mid-latitude storm tracks (Field et al., 2006; Lal and Jull, 2005). Consistent with this suggestion, the only existing ^{3}He$_{ET}$ flux estimate in the compilation of McGee and Mukhopadhyay (2013; Fig. 7) that is significantly lower than the mean comes from the only subtropical dry region site, in the northwest Arabian Sea (Marcantonio et al., 2001). The spatial variability in IDP fluxes could present an additional uncertainty in using IDPs (and ^{3}He by extension) as normalizing factors. Although there may have been some latitudinal movement of the ITCZ and the Hadley Cell during the past millennium, paleoclimate records throughout the Caribbean generally indicate that subtropical climates persisted (Burn et al., 2016). Therefore, we do not expect that the large-scale transport of IDPs from the subtropics to the extratropics was significantly altered over the past millennium.

Another possible explanation for lower-than-expected ^{3}He$_{ET}$ fluxes in our core is fractionation of the two helium isotopes during sediment transport. IDPs, the carrier phase of ^{3}He$_{ET}$, may be slightly larger than the Saharan dust grains carrying the ^{4}He$_{TERR}$ (5–20 μm for IDPs (McGee and Mukhopadhyay, 2013) versus 2.5–9 μm for far-field Saharan dust (Reid et al., 2003)). However, the two helium isotopes are accumulating at nearly the same ratio when being gently washed into the quiescent ponds as when more energetically being flooded above channel banks onto the Levee Crest (Fig. 8). The same is true during periods of low or high sediment focusing. We consider this evidence against fractionation by sediment transport and therefore our preferred explanation is regionally lower ^{3}He$_{ET}$ fluxes here in the subtropics due to atmospheric circulation.

Finally, in analogy to inferring the local input of ^{3}He$_{ET}$, we can use the ^{232}Th and ^{230}Th accumulation rates, assuming 1.3 g/m^2/yr dust input, to make an estimate of the ^{230}Th production rate on this region of the Bank, which could not be quantified *a priori* (Sec. 2). This ^{230}Th production rate works out to be 1.4 ng/m^2/yr, roughly 10 times the banktop benthic flux of ^{230}Th that Robinson et al. (2004) estimated from an analysis near Exuma Sound in the eastern Bahamas (see Fig. 1), indicating that there may be a regionality to the banktop "production" of ^{230}Th by porewater release. It

could be that on the northwestern Great Bahama Bank, there is more effective lateral transport of the benthic-sourced ^{230}Th into the Triple Goose Creek area than in the Exuma Cays. The difference may relate to contrasting groundwater hydrology between the two locations, as North Andros has significantly higher hydraulic conductivity than the Exumas on the southeastern portion of the Bank (Whitaker and Smart, 1997).

While more work needs to be done to define the absolute values of ^{230}Th and ^{3}He supply to the Bahama Bank, there is an undeniable stability in the dust proxy ratios in our cores. This stability argues against large changes in either IDP flux, ^{230}Th supply, or Saharan dust flux to our site over the covered time periods.

4.4. Implications for historical changes in North Atlantic dust deposition

Of course, bioturbation has smoothed these dust flux records, similar to a running average filter, contributing in part to the apparent stability. This is particularly true for the Pond and Beach cores (at least 400 yr filtering, based on the ^{210}Pb results discussed in Section 4.2) in which any century-scale changes will have been muted. However, the Pond core dust proxy ratios do agree where they overlap (AD 1100–1800) with those of the Levee Crest core, which is much less affected by bioturbation (60 yr filtering). Even given the age model uncertainty prior to AD 700, the three Andros records together indicate no trend in dust flux during the millennium between AD 800 and 1800, which overlaps the Medieval Climate Anomaly (MCA) and the Little Ice Age (LIA) (Mann et al., 2009). We emphasize that we cannot assign absolute dust fluxes in our results, or specify a precise time period due to age model uncertainties, but the finding of a lack of trend is robust.

During deglacial cooling events (Heinrich Stadial 1 and the Younger Dryas), the Early Holocene African Humid Period, and recent decadal scale variability, African dust appears to have been part of a coupled system involving North African aridity, trade wind intensity and subtropical North Atlantic cooling (e.g., Bradtmiller et al., 2016; Evan et al., 2011). We hypothesize that the lack of apparent changes in Bahamas dust fluxes in response to centennial-scale climate variability between 800 and 1800 AD reflects the fact that the Little Ice Age was marked by relatively warm conditions in the high-latitude North Atlantic (as opposed to the continents) (Mann et al., 2009), limiting the trade wind response. A recent study has found, however, reduced frequency of Caribbean hurricanes during the LIA, a factor possibly related to North Atlantic climate variability similar to previous cool periods (Trouet et al., 2016). Given modern correlations between African dust emissions and hurricane occurrence (Evan et al., 2006), one would expect increased dust emissions during the LIA if the Caribbean result is representative of overall hurricane activity over the North Atlantic. It may be that increased volcanic aerosol loads in the far North Atlantic during the LIA drove a climate response in which Saharan aerosol dust generation became decoupled from western Atlantic storm generation. The connection between African dust transport and Atlantic hurricane activity during the past millennium deserves further investigation from other climate archives.

On the issue of the regional impact of anthropogenic dust from the Sahel, we rely solely on the Levee Crest core. As described above, the radiocarbon and lead-210 dating in this core give us high confidence that the past 200 yr are recorded here, albeit filtered by a 60 yr running average. The dust proxy data indicate no variability over this time period outside the ~10% variations seen in the records as a whole. The bioturbation of this core would have muted the magnitude of decadal events, but any pre-industrial to modern trend in dust input would not be masked by a running average. For instance, applying a 60 yr running average to the West African dust flux record (Mulitza et al., 2010) only reduces the apparent increase in dust flux between 1800 to 2000 AD from a factor of 4 to a factor of 2.5, also not supported by our data.

Furthermore, the dissolved ^{232}Th/^{230}Th ratio in the banktop and Pond waters (average shown as a star in Fig. 8) is consistent within uncertainty with the average value in the cores. In the water samples, the measured dissolved ^{230}Th was corrected for ingrowth from the decay of dissolved U between the time of sampling and analysis, but we do not make a lithogenic correction since it is the total dissolved ^{230}Th that will adsorb onto carbonate particles, whether sourced from dust or benthic release. Because the dissolved Th ratio represents an average of dust deposition in accordance with the residence time of Th in the water (less than a year), this is another strong indication that dust flux to the Bahamas today is similar (within 10%) to the average deposition over at least the past 200 yr. We thus suggest that the onset of commercial agriculture in the Sahel did not greatly modify the transport of North African dust to the western North Atlantic. This suggestion is consistent with the understanding that Saharan sources have been the dominant contributors to the North African dust plume, with relatively minor inputs from the Sahel (Ginoux et al., 2012). This finding will be important for the modeling of aerosol fields from the pre-industrial to modern day and the choice of aerosol fields used for preindustrial and last millennium simulations. In particular, our results suggest that the use of dust fields scaled to 50% of modern levels in simulations of preindustrial climates (e.g., Albani et al., 2014) may need to be reconsidered.

5. Conclusions and future work

We have described Saharan dust proxies in a set of tidal flat cores from Andros Island, Bahamas. The chronological and geochemical work undertaken has led to several interesting avenues for future work. These are (1) to investigate areas of the Triple Goose Creek region in Andros Island that have apparent ages at 1.3 m depth of 3700 yr, despite the fact the Pleistocene cement basement here was only flooded hundreds to thousands of years before this, (2) to determine if recent extraterrestrial ^{3}He deposition to the Bahamas could be a factor of 3 lower than has been found in the Holocene sections of the Greenland and Antarctic ice cores, and (3) to determine the magnitude and spatial distribution of the benthic flux of ^{230}Th from banktop sediments into banktop waters. These puzzles notwithstanding, dust proxy data derived from the cores suggest that transport of Saharan dust to the western subtropical North Atlantic did not undergo large, factor of 4 magnitude changes from the pre-industrial period to today. Furthermore, no long term trends in dust input to the Bahamas are apparent over the past millennium. The transport of North African dust to the western Atlantic may not have participated in climate feedbacks associated with ITCZ movement over this time period.

Acknowledgements

We are grateful for the students of the 2013–2014 Princeton Sedimentology course for coring work. Sample preparation by Clio Macrakis and Ashling Neary, during their High School and undergraduate research experiences, respectively, is greatly appreciated. We are thankful for logistical support from the staff of Small Hope Bay Lodge. CTH was supported by the W.O. Crosby Postdoctoral Fellowship at MIT and by the University of Southern Mississippi. Data from this study can be accessed in the electronic supplement. We thank Franco Marcantonio, Brent Goehring, editor Martin Frank and two anonymous reviewers for thoughtful comments.

Appendix A. Supplementary material

Supplementary material related to this article can be found online at http://dx.doi.org/10.1016/j.epsl.2016.10.031.

References

Albani, S., Mahowald, N.M., Perry, A.T., Scanza, R.A., Zender, C.S., Heavens, N.G., Maggi, V., Kok, J.F., Otto-Bliesner, B.L., 2014. Improved dust representation in the community atmosphere model. J. Adv. Model. Earth Syst. 6, 541–570. http://dx.doi.org/10.1002/2013MS000279.

Albani, S., Mahowald, N.M., Winckler, G., Anderson, R.F., Bradtmiller, L.I., Delmonte, B., François, R., 2015. Twelve thousand years of dust: the Holocene global dust cycle. Clim. Past 11, 869–903. http://dx.doi.org/10.5194/cp-11-869-2015.

Bhattacharya, A., 2012. Application of the Helium Isotopic System to Accretion of Terrestial and Extraterrestial Dust Through the Cenozoic. Ph.D. dissertation. Proquest Dissertations No. 923820831. Harvard University.

Bradtmiller, L.I., McGee, D., Awalt, M., Evers, J., Yerxa, H., Kinsley, C.W., DeMenocal, P.B., 2016. Changes in biological productivity along the northwest African margin over the past 20,000 years. Paleoceanography 31, 1–18. http://dx.doi.org/10.1002/2015PA002862.

Brook, E.J., Kurz, M.D., Curtice, J., Cowbum, S., 2000. Accretion of interplanetary dust in polar ice. Geophys. Res. Lett. 27, 3145–3148. http://dx.doi.org/10.1029/2000GL011813.

Brook, E.J., Kurz, M.D., Curtice, J., 2009. Flux and size fractionation of ^{3}He in interplanetary dust from Antarctic ice core samples. Earth Planet. Sci. Lett. 286, 565–569. http://dx.doi.org/10.1016/j.epsl.2009.07.024.

Burn, M.J., Holmes, J., Kennedy, L.M., Bain, A., Marshall, J.D., Perdikaris, S., 2016. A sediment-based reconstruction of Caribbean effective precipitation during the Little Ice Age from Freshwater Pond, Barbuda. Holocene 26, 1237–1247. http://dx.doi.org/10.1177/0959683616638418.

Evan, A.T., Dunion, J., Foley, J.A., Heidinger, A.K., Velden, C.S., 2006. New evidence for a relationship between Atlantic tropical cyclone activity and African dust outbreaks. Geophys. Res. Lett. 33, 1–5. http://dx.doi.org/10.1029/2006GL026408.

Evan, A.T., Foltz, G.R., Zhang, D., Vimont, D.J., 2011. Influence of African dust on ocean – atmosphere variability in the tropical Atlantic. Nat. Geosci. 4, 762–765. http://dx.doi.org/10.1038/ngeo1276.

Evan, A.T., Flamant, C., Gaetani, M., Guichard, F., 2016. The past, present and future of African dust. Nature 531, 493–495. http://dx.doi.org/10.1038/nature17149.

Farley, K.A., Love, S.G., Patterson, D.B., 1997. Atmospheric entry heating and helium retentivity of interplanetary dust particles. Geochim. Cosmochim. Acta 61, 2309–2316. http://dx.doi.org/10.1016/S0016-7037(97)00068-9.

Field, C.V., Schmidt, G.A., Koch, D., Salyk, C., 2006. Modeling production and climate-related impacts on ^{10}Be concentration in ice cores. J. Geophys. Res. 111, D15107. http://dx.doi.org/10.1029/2005JD006410.

Francois, R., Frank, M., van der Loeff, M.M., Bacon, M.P., 2004. ^{230}Th normalization: an essential tool for interpreting sedimentary fluxes during the late Quaternary. Paleoceanography 19, PA1018. http://dx.doi.org/10.1029/2003PA000939.

Gayer, E., Mukhopadhyay, S., Meade, B.J., 2008. Spatial variability of erosion rates inferred from the frequency distribution of cosmogenic ^{3}He in olivines from Hawaiian river sediments. Earth Planet. Sci. Lett. 266, 303–315. http://dx.doi.org/10.1016/j.epsl.2007.11.019.

Ginoux, P., Prospero, J.M., Gill, T.E., Hsu, N.C., Zhao, M., 2012. Global-scale attribution of anthropogenic and natural dust sources and their emission rates based on MODIS Deep Blue aerosol products. Rev. Geophys. 50, RG3005. http://dx.doi.org/10.1029/2012RG000388.

Glaser, P.H., Hansen, B.C.S., Donovan, J.J., Givnish, T.J., Stricker, C.A., Volin, J.C., 2013. Holocene dynamics of the Florida Everglades with respect to climate, dustfall, and tropical storms. Proc. Natl. Acad. Sci. USA 110, 17211–17216. http://dx.doi.org/10.1073/pnas.1222239110.

Hardie, L.A., 1977. Sedimentation on the Modern Carbonate Tidals Flats of Northwest Andros Island, Bahamas. The Johns Hopkins University Press, Baltimore.

Hayes, C.T., Anderson, R.F., Fleisher, M.Q., Serno, S., Winckler, G., Gersonde, R., 2013. Quantifying lithogenic inputs to the North Pacific Ocean using the long-lived thorium isotopes. Earth Planet. Sci. Lett. 383, 16–25. http://dx.doi.org/10.1016/j.epsl.2013.09.025.

Henderson, G.M., Lindsay, F.N., Slowey, N.C., 1999. Variation in bioturbation with water depth on marine slopes: a study on the Little Bahamas bank. Mar. Geol. 160, 105–118. http://dx.doi.org/10.1016/S0025-3227(99)00018-3.

Klinkhammer, G.P., Palmer, M.R., 1991. Uranium in the oceans: where it goes and why. Geochim. Cosmochim. Acta 55, 1799–1806. http://dx.doi.org/10.1016/0016-7037(91)90024-Y.

Lal, D., Jull, A.J.T., 2005. On the fluxes and fates of ^{3}He accreted by the Earth with extraterrestrial particles. Earth Planet. Sci. Lett. 235, 375–390. http://dx.doi.org/10.1016/j.epsl.2005.04.011.

Maloof, A.C., Kopp, R.E., Grotzinger, J.P., Fike, D.A., Bosak, T., Vali, H., Poussart, P.M., Weiss, B.P., Kirschvink, J.L., 2007. Sedimentary iron cycling and the origin and preservation of magnetization in platform carbonate muds, Andros Island, Bahamas. Earth Planet. Sci. Lett. 259, 581–598. http://dx.doi.org/10.1016/j.epsl.2007.05.021.

Maloof, A.C., Grotzinger, J.P., 2012. The Holocene shallowing-upward parasequence of north-west Andros Island, Bahamas. Sedimentology 59, 1375–1407. http://dx.doi.org/10.1111/j.1365-3091.2011.01313.x.

Mann, M.E., Zhang, Z., Rutherford, S., Bradley, R.S., Hughes, M.K., Shindell, D., Ammann, C., Faluvegi, G., Ni, F., 2009. Global signatures and dynamical origins of the Little Ice Age and Medieval Climate Anomaly. Science 326, 1256–1260. http://dx.doi.org/10.1126/science.1177303.

Marcantonio, F., Anderson, R.F., Higgins, S., Fleisher, M.Q., Stute, M., Schlosser, P., 2001. Abrupt intensification of the SW Indian Ocean monsoon during the last deglaciation: constraints from Th, Pa, and He isotopes. Earth Planet. Sci. Lett. 184, 505–514. http://dx.doi.org/10.1016/S0012-821X(00)00342-3.

McGee, D., Mukhopadhyay, S., 2013. Extraterrestrial He in sediments: from recorder of asteroid collisions to timekeeper of global environmental changes. In: Burnard, P. (Ed.), The Noble Gases as Geochemical Tracers. Springer-Verlag, Berlin, Heidelberg, pp. 155–176.

McGee, D., DeMenocal, P.B., Winckler, G., Stuut, J.B.W., Bradtmiller, L.I., 2013. The magnitude, timing and abruptness of changes in North African dust deposition over the last 20,000 yr. Earth Planet. Sci. Lett. 371–372, 163–176. http://dx.doi.org/10.1016/j.epsl.2013.03.054.

McGee, D., Winckler, G., Borunda, A., Serno, S., Anderson, R.F., Recasens, C., Bory, A., Gaiero, D., Jaccard, S.L., Kaplan, M., McManus, J.F., Revel, M., Sun, Y., 2016. Tracking eolian dust with helium and thorium: impacts of grain size and provenance. Geochim. Cosmochim. Acta 175, 47–67. http://dx.doi.org/10.1016/j.gca.2015.11.023.

Muhs, D.R., Budahn, J.R., Prospero, J.M., Carey, S.N., 2007. Geochemical evidence for African dust inputs to soils of western Atlantic islands: Barbados, the Bahamas, and Florida. J. Geophys. Res. 112, F02009. http://dx.doi.org/10.1029/2005JF000445.

Mukhopadhyay, S., Kreycik, P., 2008. Dust generation and drought patterns in Africa from helium-4 in a modern Cape Verde coral. Geophys. Res. Lett. 35, L20820. http://dx.doi.org/10.1029/2008GL035722.

Mulitza, S., Heslop, D., Pittauerova, D., Fischer, H.W., Meyer, I., Stuut, J., Zabel, M., Mollenhauer, G., Collins, J.A., Kuhnert, H., Schulz, M., 2010. Increase in African dust flux at the onset of commercial agriculture in the Sahel region. Nature 466, 226–228. http://dx.doi.org/10.1038/nature09213.

Niang, A.J., Ozer, A., Ozer, P., 2008. Fifty years of landscape evolution in Southwestern Mauritania by means of aerial photos. J. Arid Environ. 72, 97–107. http://dx.doi.org/10.1016/j.jaridenv.2007.04.009.

Preiss, N., Genthon, C., 1997. Use of a new database of lead 210 for global aerosol model validation. J. Geophys. Res. 102, 347–357. http://dx.doi.org/10.1029/97JD01389.

Prospero, J.M., 1999. Long-term measurements of the transport of African mineral dust to the southeastern United States: implications for regional air quality. J. Geophys. Res. 104, 15917–15927. http://dx.doi.org/10.1029/1999JD900072.

Prospero, J.M., Lamb, P.J., 2003. African droughts and dust transport to the Caribbean: climate change implications. Science 302, 1024–1027. http://dx.doi.org/10.1126/science.1089915.

Prospero, J.M., Nees, R.T., Uematsu, M., 1987. Deposition rate of particulate and dissolved aluminum derived from Saharan dust in precipitation at Miami, Florida. J. Geophys. Res. 92, 14723–14731. http://dx.doi.org/10.1029/JD092iD12p14723.

Prospero, J.M., Landing, W.M., Schulz, M., 2010. African dust deposition to Florida: temporal and spatial variability and comparisons to models. J. Geophys. Res. 115, D13304. http://dx.doi.org/10.1029/2009JD012773.

Reid, J.S., Jonsson, H.H., Maring, H.B., Smirnov, A., Savoie, D.L., Cliff, S.S., Reid, E.A., Livingston, J.M., Meier, M.M., Dubovik, O., Tsay, S.C., 2003. Comparison of size and morphological measurements of coarse mode dust particles from Africa. J. Geophys. Res., Atmos. 108, 8593. http://dx.doi.org/10.1029/2002JD002485.

Robinson, L.F., Belshaw, N.S., Henderson, G.M., 2004. U and Th concentrations and isotope ratios in modern carbonates and waters from the Bahamas. Geochim. Cosmochim. Acta 68, 1777–1789. http://dx.doi.org/10.1016/j.gca.2003.10.005.

Rodríguez, S., Cuevas, E., Prospero, J.M., Alastuey, A., Querol, X., García, M.I., 2015. Modulation of Saharan dust export by the North African dipole. Atmos. Chem. Phys. 15, 7471–7486. http://dx.doi.org/10.5194/acp-15-7471-2015.

Shanahan, T.M., Mckay, N.P., Hughen, K.A., Overpeck, J.T., Otto-bliesner, B., Heil, C.W., King, J., Scholz, C.A., Peck, J., 2015. The time-transgressive termination of the African Humid Period. Nat. Geosci. 8, 140–144. http://dx.doi.org/10.1038/NGEO2329.

Shinn, E.A., Lloyd, R.M., Ginsburg, R.N., 1969. Anatomy of a modern carbonate tidal-flat. J. Sediment. Petrol. 39, 1202–1228. http://dx.doi.org/10.1306/74D71DCF-2B21-11D7-8648000102C1865D.

Slowey, N.C., Henderson, G.M., 2011. Radiocarbon ages constraints on the origin and shedding of bank-top sediment in the Bahamas during the Holocene. Aquat. Geochem. 17, 419–429. http://dx.doi.org/10.1007/s10498-011-9140-5.

Trouet, V., Harley, G.L., Domínguez-Delmás, M., 2016. Shipwreck rates reveal Caribbean tropical cyclone response to past radiative forcing. Proc. Natl. Acad. Sci. USA 113, 3169–3174. http://dx.doi.org/10.1073/pnas.1519566113.

Tsigaridis, K., Krol, M., Dentener, F.J., Balkanski, Y., Lathière, J., Metzger, S., Hauglustaine, D.a., Kanakidou, M., 2006. Change in global aerosol composition since preindustrial times. Atmos. Chem. Phys. 6, 5143–5162. http://dx.doi.org/10.5194/acp-6-5143-2006.

Turekian, K.N., Benninger, L.K., Dion, E.P., 1983. ^{7}Be and ^{210}Pb total deposition fluxes at New Haven, Connecticut and at Bermuda. J. Geophys. Res. 88, 5411–5415. http://dx.doi.org/10.1029/JC088iC09p05411.

Weldeab, S., Lea, D.W., Schneider, R.R., Andersen, N., 2007. 155,000 years of West African monsoon and ocean thermal evolution. Science 316, 1303–1307. http://dx.doi.org/10.1126/science.1140461.

Whitaker, F.F., Smart, P.L., 1997. Hydrogeology of the Bahamian Archipelago. In: Vacher, H.L., Quinn, T. (Eds.), Geology and Hydrogeology of Carbonate Islands. In: Dev. Sedimentol., vol. 54. Elsevier Science, pp. 183–216.

Williams, R.H., McGee, D., Kinsley, C., Ridley, D.A., Hu, S., Federov, A., Tal, I., Murray, R.W., DeMenocal, P.B., in press. Glacial to Holocene changes in trans-Atlantic Saharan dust transport and dust-climate feedbacks. Sci. Adv. http://dx.doi.org/10.1126/sciadv.1600445.

Winckler, G., Fischer, H., 2006. 30,000 years of cosmic dust in Antarctic Ice. Science 80 (313), 491. http://dx.doi.org/10.1126/science.1127469.